energy&fuels

ARTICLE

pubs.acs.org/EF

A Study on Coal Properties and Combustion Characteristics of Blended Coals in Northwestern China

Chang'an Wang, Yinhe Liu, Xiaoming Zhang, and Defu Che*

State Key Laboratory of Multiphase Flow in Power Engineering, School of Energy and Power Engineering, Xi'an Jiaotong University, Xi'an 710049, China

ABSTRACT: The utilization of blended coals has become popular in northwestern China. In this paper, investigations on coal properties and combustion characteristics of blended coals have been carried out to provide guidance for blended-coal-fired plants. Experimental results show that proximate, ultimate, and calorific value analyses of blended coals can be calculated by mass-weighted average of individual coals. However, grindability, ash composition, ash fusion temperatures, and some characteristics related to combustion performance of blended coals cannot be predicted accurately from those of individual coals and the mixture ratio. Blending a coal of high fusion temperatures with a coal of low fusion temperatures can significantly increase the ash fusion temperatures of blended coals. Thermogravimetric experimental results indicate that the intense combustion stage of blended coals is quite different from those of individual coals. Thermogravimetric curves of blended coals lie between those of individual coals but show nonadditive behavior. Furthermore, combustion characteristics of blended coals improve significantly with increased oxygen concentration, and combustion performance of low-reactivity coal is less sensitive to changes in oxygen concentration. Kinetic analysis indicates that the apparent activation energy of coal combustion is not constant at different conversion fractions. The combustion process of blended coals is charactered by segmentation and the apparent activation energy in low-temperature zone is higher than that in high-temperature zone. The mean activation energy of blended coals shows nonadditivity performance in both Kissinger−Akahira−Sunose (KAS) and Coats−Redfern methods due to the interaction between individual coals. The KAS method is more adequate than the Coats−Redfern method for analyzing the kinetics of blended coal combustion because the Coats−Redfern method requires prior assumption of reaction mechanism and its analysis results sometimes differ clearly from experimental results.

1. INTRODUCTION

China is one of the largest energy consumers in the world, and coal accounts for the main part of China's energy consumption nowadays.[1] Current energy forecasts indicate that the future energy consumption of China will still largely rely on coal. Therefore, many researchers devote themselves to the study of coal combustion. Because of the tight supply situation and rising price of coals, the actual coals used in coal-fired power plants of China are usually significantly different from the design coal, which may seriously deteriorate the safety and economy of power plants. Blended coal combustion technology has been proved an effective method to increase fuel flexibility, improve the performance of coals, extend the range of acceptable coals, and meet specifications of power plants.[2,3] However, the behavior of blended coals may differ greatly from the expected pattern due to some nonadditive properties of coal parameters. Hence, it is of crucial importance to understand the combustion characteristics of blended coals to guide the operation of blended-coal-fired plants.

There have been a number of investigations on utilization of blended coals. These investigations include ignition behavior of blended coals,[4,5] petrology and reactivity of blended coals,[6] emission characteristics of gaseous pollutants[7,8] and mineral particles,[9,10] blended coal model,[11,12] and so on. However, sometimes the results obtained by different researchers are quite different, usually due to differences in the properties of individual coals used. Although some power plants have fired blended coals successfully based on operation experiences, the underlying mechanisms of blended coal combustion are still poorly understood. On the other hand, differences of Chinese coal properties are too great and little attention has been paid to blended coals in northwestern China. The existing research results could not guide the utilization of blended coals scientifically and accurately in this region due to the complexity of blended coal combustion. In this paper, our investigation is specific to blended coals in northwestern China and is beneficial to enrich the database on blended coal combustion in China.

Coal analysis, such as proximate and ultimate analyses and determination of net calorific value, is essential for boiler design and retrofitting. Therefore, the understanding and prediction of blended coal properties are important for reasonable retrofitting and safe operation of boilers. Grindability of coal has a significant effect on the output of coal pulverizer, which can influence the cycle efficiency of the power plant.[13,14] Nevertheless, there are no consistent results on grindability of blended coals. Slagging tendency of fuel in boilers is one of the main factors that influence the boiler safety. Slagging often occurs in the plants that burn coals with low fusion temperatures. At present, many plants are mixing low and high fusion temperature coals to relieve the problem of slagging and coking in northwestern China.

Received: May 6, 2011
Revised: July 7, 2011
Published: July 11, 2011

Table 1. Proximate and Ultimate Analyses of Coal

		proximate analysis (wt %, ad)				ultimate analysis (wt %, ad)					
coal code	fuel ratio	w(FC)	w(A)	w(V)	w(M)	w(C)	w(H)	w(O)[a]	w(N)	w(S)	$Q_{net,ar}$ (MJ·kg^{-1})
LX	1.79	46.09	18.19	25.70	10.02	57.40	3.03	10.1	0.93	0.33	19.76
XJ	2.30	55.83	14.70	24.28	5.19	65.82	3.00	6.77	0.84	3.68	23.20
ZQ	1.98	46.09	20.62	23.32	9.97	55.69	2.64	9.70	0.78	0.60	19.71
QC	2.54	45.97	35.16	18.12	0.75	54.94	3.1	4.61	1.09	0.35	19.76
JH	2.04	43.14	34.66	21.17	1.03	53.76	3.21	5.73	0.93	0.68	19.11
HX	1.50	38.76	32.80	25.84	2.60	51.41	3.19	7.17	0.97	1.86	18.78

[a] $w(O) = 100 - w(C) - w(H) - w(N) - w(S) - w(A) - w(M)$.

Nevertheless, coals are blended just by experience in most plants. Therefore, this work is concerned with presenting coal properties of blended coals in northwestern China to predict possible deviations from the expected results.

Research on coal combustion can be conducted in full-scale boilers or pilot-scale facilities or with laboratory-scale equipment. Thermogravimetric analysis is a simple and practicable approach and has been widely used to study combustion and kinetic characteristics of coals.[15−21] It has been confirmed that the conclusions drawn by thermogravimetry can provide an important reference for operation of a boiler firing blended coal. Hence, thermogravimetry has also been applied to investigate the combustion characteristics of representative individual coals and blended coals in northwestern China. In this paper, research on blended coals is systematic and comprehensive, including coal properties, slagging properties, combustion characteristics, and kinetics analysis. Study on combustion performance of blended coals at low oxygen concentration has been also performed, which is still very insufficient in recent investigations. Moreover, both a single heating rate method (the Coats−Redfern method) and an isoconversional method (the Kissinger-Akahira-Sunose method) are contrastively employed to carry out the kinetic analysis of blended coal combustion. The results of this study are of great importance to enhance the understanding of the characteristics of blended coals and also to provide specific guidance for further design and operation of blended-coal-fired plants in northwestern China.

2. EXPERIMENTAL SECTION

2.1. Coal Analysis. Six types of coals were selected for this study, including Lingxin bituminous (abbreviated as LX hereafter), Xinjing bituminous (XJ), Zaoquan bituminous (ZQ), Qiancheng bituminous (QC), Juhui bituminous (JH), and Huaxin lignite (HX). All these coals are typical in northwestern China. Each sample was first ground, sieved to size 100−125 μm, and then dried at 105 °C and kept airproof in a glass container at room temperature before being used. The coal samples studied in this research were prepared following ISO Standards [ISO 18283:2006(E)]. The proximate and ultimate analyses and net calorific value of coal samples are listed in Table 1, in which all coals are represented as the corresponding code names. In Table 1, the proximate and ultimate analyses are both on air-dry basis, indicated as ad in this paper. Fuel ratio is defined as the ratio of fixed carbon content to volatile content (FC_{daf}/V_{daf}) and can be used as an indicator of coal rank.[22] Fuel ratios of coals selected for this study range quite widely between 1.50 and 2.54, as shown in Table 1.

2.2. Experimental Method. Hardgrove grindability index (HGI) has been widely used to identify the grindability of coal because of the simple, quick operation and the good reproducibility of its measurement. Although the method for characterizing the ash fusibility may vary considerably from country to country, the ash fusion temperatures are obtained in the same way, by observing the behavior of the ash that has in advance been put into a prescribed shape when heated progressively under strictly prescribed conditions. The popular pyramid method, which is internationally widely used, is applied to measure the ash fusibility of blended coals in this study. Intelligent ash fusibility analyzer 5E-AFIII with computer image recognition technology is employed to determine the four characteristic temperatures: deformation temperature (abbreviated as DT hereafter), softening temperature (ST), hemispherical fusion temperature (HT), and fluid temperature (FT).

Nonisothermal thermogravimetry is used in the combustion experiments on both individual coal and blended coal. In the experiments, 10 ± 0.1 mg of coal sample is first weighed on a Sartorius MC5-type electronic balance at the microgram level; the coal sample is then put it into an Al_2O_3 container and the container is placed in the Netzsch simultaneous thermal analyzer STA 409 PC. All the experiments are carried out in the temperature range 25−1200 °C with a preset O_2−N_2 gas flow rate of 100 mL·min^{-1}. The temperature rises linearly at heating rates of 10, 15, 20, and 30 °C·min^{-1}. Prior to the experiments, the thermogravimetry instrument is calibrated for both temperature reading and buoyancy effect. All the experiments were performed at least twice for repeatability.

3. RESULTS AND DISCUSSION

3.1. Coal Properties of Blended Coals. *3.1.1. Proximate and Ultimate Analyses and Calorific Values of Blended Coals.* Proximate and ultimate analyses and calorific value of coals are of great importance in design, check, performance testing, and combustion control of a boiler. Accurate prediction of coal characteristics of blended coals from those of individual coals is quite significant to ensure the reliable and economic operation of a blended-coal-fired power plant.

Blended coal samples are composed of ground individual coals. All the blended coals are analyzed in the same way as the individual coals. It can be observed from ultimate analysis of individual and blended coals that carbon, hydrogen, sulfur, and nitrogen contents vary almost linearly with the mixture ratio. Furthermore, the measured data agree well with the calculated weighted average results. The relative deviation is less than 5%. However, the experimental value of oxygen content in blended coal deviates greatly from the calculated result. Because oxygen content is calculated by a subtraction method, the calculated result will be inclusive of the errors of C, H, N, S, moisture, and ash measurements. It is an approximate value with low accuracy. Therefore, elemental contents of blended coal can be calculated by mass-weighted average of individual coals. This conclusion is consistent with that achieved by Riley et al.[23]

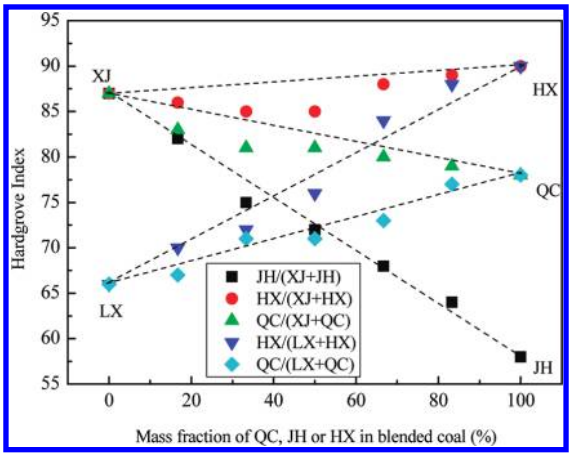

Figure 1. HGIs of blended coals vs mixture ratio.

Apart from ultimate analysis, proximate analysis and calorific values of blended coals were also studied in this paper. It also can be noted that there are no significant deviations observed between calculated and measured results of ash, fixed carbon, moisture and volatile matter content. Hence, the proximate analysis of blended coals shows additive behavior. $Q_{b,ad}$ represents the bomb calorific value, which is measured in an oxygen bomb calorimeter. $Q_{net,ar}$ represents the net calorific value, which is a calculated value and is usually used in the heat balance calculations of boilers in China. Moreover, $Q_{b,ad}$ and $Q_{net,ar}$ of blended coal are both in agreement with the results calculated by weighted average.

3.1.2. Grindability of Blended Coals. The coal combustion characteristics and thermal efficiency of power plant are significantly affected by both particle size and its distribution of pulverized coal. In the blended-coal-fired power plants of northwestern China, individual coals are usually blended before entering the mill in order to reduce equipment investment. As a result, the effect of hardness difference between individual coals on mill operation should be considered. The effects of hardness and coal rank of the individual coals on the HGIs of blended coals were also studied in this paper. HGI data of typical individual coals and blended coals are shown in Figure 1. Coals XJ and HX are soft coals,with HGI values of 87 and 90, respectively, while coal JH is a hard coal with an HGI of 58. In addition, the hardness values of coals QC and LX are moderate, with corresponding HGI values of 78 and 66 respectively. According to the literature,[24] the maximum allowable deviation of HGI values among the measured HGI results of repeated experiments is 2 in the same laboratory. Therefore, if the absolute deviation between measured data and calculated result is equal or less than 2, the HGIs of blended coals could be considered to follow the additivity rule.

It can be seen from Figure 1 that the change in blended coal grindability is quite complicated. Grindability of some coals follows the linear additivity rule. The HGIs of blended coals composed of XJ/JH or LX/QC are in agreement with the results of mass-weighted average, as shown in Figure 1, which is consistent with that obtained by Vuthaluru et al.[13] However, it is apparent that there is a preferential shift of the HGIs of blended coals XJ/QC or XJ/HX toward lower values, relative to those expected from the linear additivity rule. For XJ/QC or XJ/HX, the grindabiliy of blended coals is close to that of the hard individual coals, which is consistent with the result observed by Zhong and Qiu[25] but differs from the conclusion obtained by Rubiera et al.[14] It could be concluded that, on the whole, the HGIs of blended coals could not be predicted from the HGIs of individual coals and mixture ratio. Experiments are necessary to determine the HGIs of blended coals. As for the particle size distribution of individual coals in blended pulverized coal, the size of hard coal is larger, while the size of soft coal is smaller. Hence, the burnout performance of hard individual coal in blended coals will get worse because of the increase of hard coal particle size.

3.1.3. Composition of Blended Coal Ash. Composition of ash has a considerable effect on slagging properties during coal combustion. Ash fusion temperatures of individual coals depend mainly on the contents of various oxides in the ash. The basic oxides including CaO, MgO, Fe_2O_3, K_2O, and Na_2O usually reduce the ash fusion temperatures of coals. However, because various ash components of individual coals would interact greatly in blended coal combustion, the slagging properties of blended coal ash would be much more complicated.

Four groups of representative blended coals are chosen to investigate the change of ash composition with mixture ratio and to analyze the mechanism and principle of slagging properties of blended coals, which can supply guidance to relieve or prevent slagging. It can be seen from Table 2 that all the ash compositions of blended coals display nonadditive effects, possibly due to both interactive effects between various ash components and the transformation of various oxides. Therefore, experiments are still necessary. The deviation between experimental data and calculated results increases dramatically when the disparity of ash components between individual coals rises. Some of the ash composition content of blended coal does not lie between the corresponding contents of the two individual coals, as shown in Table 2. Furthermore, the ash composition of blended coals changes quite differently with the mixture ratio. For most blended coals, the content of SiO_2 is higher than that calculated from the linear additive rule, while the change of Fe_2O_3 content is just opposite. In addition, Fe_2O_3 content of 75% blended coal samples is lower than that of either of the two individual coals. Thus, the weighted average should not be used to predict the Fe_2O_3 content of blended coals.

From Table 2, it can also be noted that the Al_2O_3, MgO, TiO_2 and K_2O contents of blended coals all lie between those of the corresponding individual coals but are not consistent with the linearly weighted average. The contents of MnO_2 and CaO in most blended coals are lower than that calculated by the weighted-average method. All the measured results of Na_2O in blended coals show positive deviations with respect to the calculated data, which would cause a decrease in ash fusion temperatures of blended coals.

It is more difficult to predict the slagging tendency in a blended-coal-fired boiler accurately because of the complicated change of ash composition of blended coals. In some cases, combustion performance testing is necessary to determine the slagging tendency during blended coal combustion.

3.1.4. Ash Fusion Temperatures of Blended Coal. Slag is formed mainly because the ash particles entrained in flue gases, which are fused or partly fused, are cooled and resolidified when they impinge on furnace walls, water-cooled walls, or tubes. Experimental results show that slagging would occur in the power plants that burn coals LX, XJ, or ZQ in northwestern China because of the high content of basic oxides and low ash fusion temperature, as shown in Tables 2 and 3. It was reported

Table 2. Composition Analysis of Blended Coal Ash

mixture ratio	SiO_2 (wt %)	Al_2O_3 (wt %)	TiO_2 (wt %)	Fe_2O_3 (wt %)	CaO (wt %)	MgO (wt %)	K_2O (wt %)	Na_2O (wt %)	MnO_2 (wt %)	SO_3 (wt %)
					LX/QC Blends					
LX	56.88	20.16	1.24	8.03	3.54	2.35	1.32	0.13	0.07	2.37
LX/QC = 2:1	54.49	33.29	1.56	3.80	2.41	1.39	0.91	0.2	0.03	1.55
LX/QC = 1:1	50.36	36.48	1.67	2.64	2.21	1.00	0.53	0.08	0.02	1.42
LX/QC = 1:2	50.76	34.7	1.48	2.59	2.6	0.74	0.58	1.10	0.01	1.07
QC	43.37	42.96	1.76	4.03	1.23	0.24	0.30	0.01	0.02	0.75
					LX/HX Blends					
LX	56.88	20.16	1.24	8.03	3.54	2.35	1.32	0.13	0.07	2.37
LX/HX = 2:1	56.88	22.59	1.28	5.50	3.50	2.53	1.06	0.15	0.04	2.70
LX/HX = 1:1	50.94	29.08	1.33	5.52	2.92	2.22	0.82	0.15	0.04	2.80
LX/HX = 1:2	53.44	29.82	1.46	4.76	2.98	1.09	0.76	0.12	0.05	3.15
HX	51.16	30.15	1.37	6.88	2.72	0.64	0.52	0.01	0.06	2.74
					XJ/QC Blends					
XJ	33.33	19.98	1.10	15.6	8.52	6.28	0.80	0.33	0.46	10.02
XJ/QC = 2:1	44.78	34.66	1.54	5.82	4.23	2.17	0.67	0.23	0.21	4.17
XJ/QC = 1:1	43.48	43.03	1.64	3.18	2.22	0.93	0.47	0.22	0.07	2.15
XJ/QC = 1:2	46.96	34.4	1.52	4.54	2.90	1.58	0.55	0.15	0.14	3.00
QC	43.37	42.96	1.76	4.03	1.23	0.24	0.30	0.01	0.02	0.75
					XJ/HX Blends					
XJ	33.33	19.98	1.10	15.6	8.52	6.28	0.80	0.33	0.46	10.02
XJ/HX = 2:1	48.99	26.65	1.31	7.14	4.91	2.58	0.83	0.31	0.27	4.97
XJ/HX = 1:1	51.45	29.01	1.45	6.05	4.03	1.98	0.82	0.20	0.20	4.62
XJ/HX = 1:2	48.26	26.29	1.44	7.88	3.94	2.56	0.73	0.14	0.14	3.52
HX	51.16	30.15	1.37	6.88	2.72	0.64	0.52	0.01	0.06	2.74

Table 3. Ash Fusion Temperatures[a] of Studied Coals

	LX	XJ	ZQ	JH	QC	HX
DT (°C)	1230	1220	1210	>1500	>1500	>1500
ST (°C)	1260	1260	1220	>1500	>1500	>1500
HT (°C)	1270	1280	1240	>1500	>1500	>1500
FT (°C)	1330	1320	1300	>1500	>1500	>1500

[a] DT, deformation temperature; ST, softening temperature; HT, hemispherical fusion temperature; FT, fluid temperature.

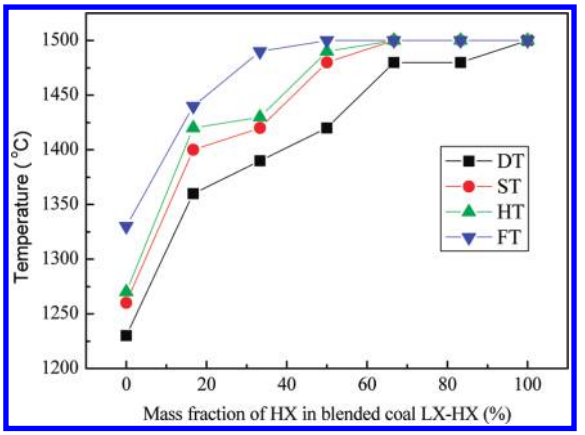

Figure 2. Analysis curves of ash fusion temperatures of blended coal LX/HX.

that coal blending could relieve slagging. However, the effects of coal blending on power plant ash slagging performance are still poorly understood. Hence, blended coals have been studied in this paper to see if they increase the ash fusion temperatures and relieve slagging. Table 3 shows all the ash fusion temperatures of the coals studied.

Ash fusion temperatures are most widely used to evaluate the slagging tendency during coal combustion. In this paper, the intelligent ash fusibility analyzer is mainly used in experimental study to measure the ash fusibility of 54 kinds of blended coals at high temperature, including coal blends with individual coals of low and high fusion temperatures and blends of both low or both high fusion temperatures.

As shown in Figure 2, when the ash fusion temperatures are higher than 1500 °C, we use 1500 °C to describe the ash fusion temperatures in graph. It can be seen from Figure 2 that ash fusion temperatures of blended coals increase significantly by blending coal of high fusion temperature into coal of low fusion temperature. However, ash fusion temperatures of blended coals cannot be predicted from those of individual coals and mixture ratio. This results from the intense interaction of various mineral matters in blended coals. Ash fusion temperatures of XJ are almost the same as those of coal LX, as shown in Table 3. Nevertheless, ash fusion temperatures of blended coals XJ/HX are quite different from those of blended coals LX/HX even if the mixture ratio is the same. The experimental results show that when the mass fraction of coal HX in blended coal XJ/HX is 16.7 wt %, the ash softening temperature of blended coal exceeds 1390 °C. However, until the content of coal HX in blended coal LX/HX increases to 50 wt %, the ash softening temperature of

dx.doi.org/10.1021/ef200686d |*Energy Fuels* 2011, 25, 3634–3645

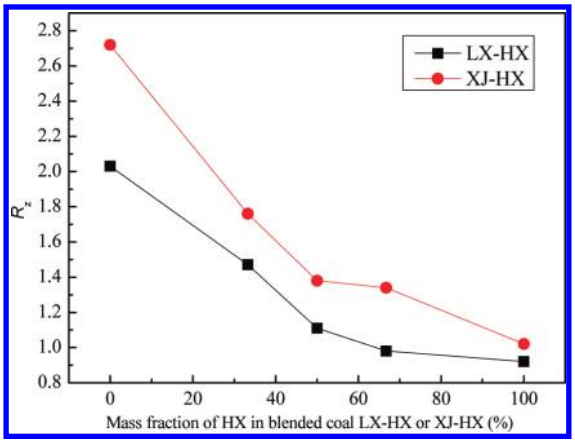

Figure 3. Change of slagging index R_z of blended coals.

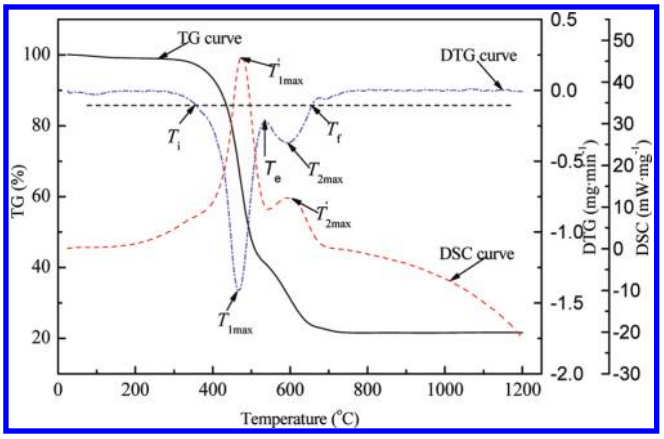

Figure 4. Thermogravimetric analysis curves of typical blended coal combustion.

blended coals could reach 1390 °C. This is because the ash composition content of coal XJ is quite different from that of coal LX, especially the content of SiO_2 and Al_2O_3.

The experimental results also show that blending of two low fusion temperature coals can lead to lower fusion temperature than either of the individual coals and cause more serious slagging problems. However, there is no slagging problem when coals whose fusion temperatures all exceed 1500 °C are blended.

In addition to ash fusion temperatures, there are many other indices used in China to judge the slagging tendency of coal ash, such as the contents of Na_2O, CaO, and Fe_2O_3, base/acid ratio B/A, silica/alumina ratio (SiO_2/Al_2O_3), ash viscosity and comprehensive index R_z. The judgment accuracy and operation complexity are quite different for different indices. McLennan et al.[26] proposed an index to indicate ash deposition and slagging potential for high iron coals, which is a typical situation in North America and the United Kingdom. Lawrence et al.[27] developed a new slagging index based on thermomechanical analysis to assess slagging propensity of Indian coals, which offers a reliable correlation with the reported slagging intensities in the field. Plaza et al.[28] used a thermodynamic model to predict the ash behavior of coals and obtain correlations that can be used to assess the strength of sintered deposits. However, the slagging indices established for particular types of coals in other countries may not necessarily be reliable when they are extended to Chinese coals. Puhua coal combustion technology center of China has compared the optimal segmentation results of typical Chinese coals with the practical slagging conditions obtained from a power plant survey. The comparison results show that the comprehensive index R_z has the highest accuracy of 90%, while the accuracy of ash fusion temperature is 83%.[29] Hence, the comprehensive index R_z is also used to analyze the slagging tendency of blended coal combustion in this paper. R_z is calculated as follows:

$$R_z = 1.24(B/A) + 0.28(w_{SiO_2}/w_{Al_2O_3}) - 0.0023ST - 0.019G + 5.42 \quad (1)$$

where

$$B/A = \frac{w_{Fe_2O_3} + w_{MgO} + w_{CaO} + w_{Na_2O} + w_{K_2O}}{w_{SiO_2} + w_{Al_2O_3} + w_{TiO_2}}$$

and

$$G = 100 \times w_{SiO_2}/(w_{SiO_2} + w_{Fe_2O_3} + w_{CaO} + w_{MgO})$$

Figure 3 shows the change of comprehensive index R_z of blended coals. It can be noted from Figure 3 that R_z decreases gradually with the increase of high fusion temperature coal HX, which indicates that the slagging degree reduces. Such a result is consistent with the practical experience of blended-coal-fired plants. However, obtaining the index R_z will consume huge manpower and material resources because both ash composition and ash fusion temperatures are needed to calculate the index R_z. Hence, ash fusion temperatures are first recommended to determine the slagging tendency of blended coal combustion during engineering practice, considering both the accuracy and complexity of measurement.

3.2. Combustion Characteristics of Blended Coal. *3.2.1. Determination of Characteristic Temperatures.* The ignition and burnout temperatures are two main characteristic temperatures that represent combustion characteristics of coal.[30] Several methods can be used to determine the ignition and burnout temperatures according to thermogravimetric analysis curves.[15,16,18,31] The temperature values obtained from different methods are usually slightly different. However, the experimental results can be compared quantitatively to some extent as long as a consistent definition of these temperatures is used. In this study, the ignition temperature T_i is defined as the temperature at which the combustion rate rises to 1 wt %·min^{-1} at the start of a major combustion process. The burnout temperature T_b is defined as the temperature at which the combustion rate diminishes to 1 wt %·min^{-1} at the end of a major combustion process.[15] As shown in Figure 4, the dashed straight line corresponds to a combustion rate of 1 wt %·min^{-1}, which is 0.1 mg·min^{-1} in this experiment. T_{1max} and T_{2max} are the temperatures corresponding to the first and peaks of the derivative thermogravimetric (DTG) curve. In addition, T'_{1max} and T'_{1max} are the temperatures corresponding to the first and second peak points of the differential scanning calorimetric (DSC) curve respectively. The temperature corresponding to the inflection point of the first and second DTG peaks is expressed as T_e.

3.2.2. Interaction Effect of Blended Coal Combustion. There are 51 kinds of blended coals mixed from six types of individual coals studied by thermogravimetric combustion experiments. It can be seen from Figure 5 that, similar to individual coal

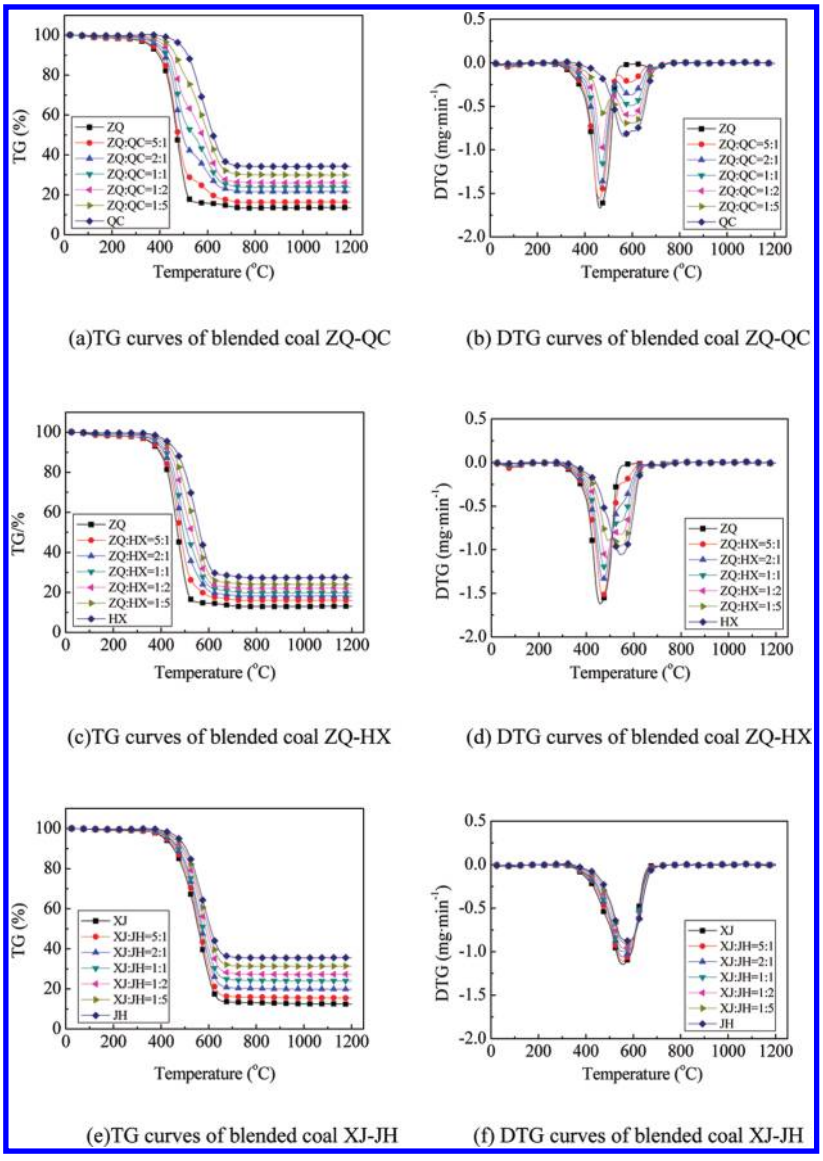

Figure 5. Thermogravimetric analysis curves of representative blended coals at heating rate of 20 °C·min^{-1}.

combustion, combustion of blended coals also occurs in three main stages: initial, intense combustion, and burnout stages. The initial stage generally involves a drying process below 300 °C, in which the TG curves are very flat due to predrying of coals. During the burnout stage, combustion has finished with almost no mass loss. In the intense combustion stage, volatile matter is first released and is ignited with subsequent coke burning, during which the mass of the coal sample is reduced rapidly and much heat is released. The initial and burnout stages of blended coals are similar to those of individual coals. However, the intense combustion stage is quite different between blended coals and individual coals. The thermogravimetric analysis curves of blended coals can be classified into three types because the combustion independence and interaction effects of individual coals differ significantly for different blended coals in the intense combustion stage. One type of thermogravimetric curve exhibits two obvious stages on TG curves of the intense combustion stage and two obvious peaks on DTG curves, as shown in Figure 5a,b. Another type shows only one stage on TG curves and one peak on DTG curves, as shown in Figure 5e,f. The third type of thermogravimetric curve is between those two types, as shown in Figure 5c,d. Because the disparities of fuel ratio and volatile matter content between the two corresponding individual coals in blended coals exhibiting two combustion stages are much larger than those in blended coals with one reaction region, TGA curves of blended coal combustion are more likely to exhibit two reaction stages if properties of one corresponding individual coal differ greatly from those of the other.

All the thermogravimetric curves of blended coals lie between those of the corresponding individual coals, but not all are consistent with additive behavior. Thermogravimetric curves of blended coals tend to be closer to the results of mass-weighted average with the combustion difference of individual coals decreasing because the interaction of the corresponding individual coals is slightly weak and individual coals would maintain combustion independence when the reactivity of individual coals is similar. In addition, both volatile matter and ash contents have considerable effect on thermogravimetric curves of blended coals. Compared with blended coal ZQ/JH of the same mixture ratio, TG and DTG curves of blended coal ZQ/HX obviously

Table 4. TG/DTG Results of Representative Blended Coals at Heating Rate of 20 °C·min^{-1}

coal sample	reaction region intervals (°C)	T_{max} (°C)	T_e (°C)	$(dw/dt)_{max}$ (mg·min^{-1})	mass loss (%)
ZQ	334−536	462.9		1.6478	84.93
ZQ/QC = 5:1	344−640	459.4	543	1.5619	82.15
ZQ/QC = 2:1	356−657	466.7	536	1.4121	77.44
ZQ/QC = 1:1	366−666	471.0	534	1.1731	75.34
ZQ/QC = 1:2	381−674	470.8	520	0.9935	73.36
ZQ/QC = 1:5	405−682	476.7	508	0.6937	69.90
QC	447−688	562.5		0.8425	65.77
ZQ	334−536	458.7		1.6478	85.19
ZQ/HX = 5:1	341−595	469.2	555	1.5294	82.03
ZQ/HX = 2:1	347−607	469.3	540	1.3463	80.69
ZQ/HX = 1:1	356−615	476.3	534	1.2013	79.06
ZQ/HX = 1:2	364−620	483.9	522	1.1026	77.45
ZQ/HX = 1:5	374−627	491.7	512	0.9633	75.53
HX	390−630	545.7		1.0549	72.35
XJ	382−650	556.9		1.1451	86.77
XJ/JH = 5:1	389−654	556.5		1.1069	83.66
XJ/JH = 2:1	396−657	556.4		1.0591	79.56
XJ/JH = 1:1	401−660	555.3		0.9977	75.58
XJ/JH = 1:2	410−665	564.9		0.9648	72.57
XJ/JH = 1:5	425−666	568.0		0.9056	68.38
JH	440−668	574.0		0.8752	64.21

tend toward lower temperature zone as shown in Figure 5. As a result, the combustion process of blended coal is conducted much more easily if the volatile matter content is higher. Figure 5 also shows that combustion process of coal JH is clearly behind that of coal XJ, although the difference of volatile matter between XJ and JH is slight. This is attributed to the ash content of coal JH being much higher than that of coal XJ.

When blended coals whose DTG curves present two peaks are considered, as shown in Figure 5b,d, the first peak corresponds to the maximum combustion rate R_{1max} of the high-reactivity coal and the second peak corresponds to the maximum combustion rate R_{2max} of the low-reactivity coal. R_{1max} decreases and R_{2max} increases with increasing content of low-reactivity coal. However, both R_{1max} and R_{2max} show nonadditive behavior.

It can also be seen from Figure 5 that T_{1max} of blended coals increases with the content of low-reactivity coal because the interaction effect of individual coals delays the combustion process of high-reactivity coal. T_{2max} of blended coals is always higher than the DTG peak temperature of low-reactivity coal burning individually. This may be attributed to the competition for oxygen between high- and low-reactivity coal. Oxygen is consumed first by high-reactivity coal, which causes the combustion rate of low-reactivity coal decrease. In addition, T'_{1max} is higher than T_{1max}, together with T'_{2max} being higher than T_{2max}. The heat release process of blended coals in thermogravimetry is a little later than the combustion process. Thermogravimetric experiments also indicate that the content of residual ash changes linearly with the mixture ratio, which is consistent with proximate analysis.

Table 4 shows the reaction region intervals, peak temperatures, inflection temperatures, maximum combustion rates, and

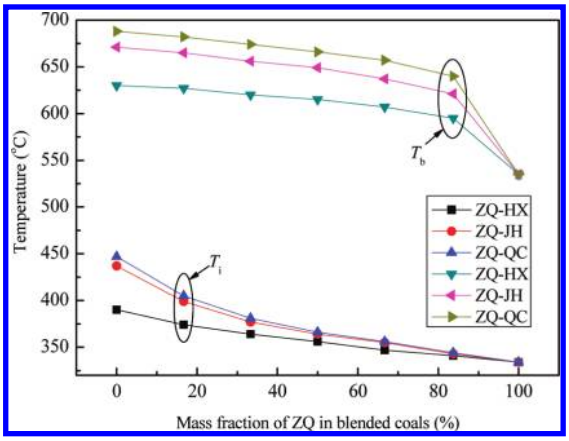

Figure 6. Ignition and burnout temperatures of blended coals at heating rate of 20 °C·min^{-1}.

mass loss of the representative blended coals at heating rate of 20 °C·min^{-1}.

As shown in Figure 6, coal ZQ is a high-reactivity coal in all three types of blended coals. Both ignition and burnout temperatures of blended coals show a decreasing trend with increasing proportion of high-reactivity coal. Moreover, when the content of high-reactivity coal begins to increase, the ignition temperatures of blended coals are reduced obviously but the burnout temperatures decrease slowly. In contrast, the ignition temperatures of blended coals change slightly but the burnout temperatures decrease sharply when the proportion of high-reactivity coal changes from 80 to 100 wt %. Hence, the ignition performance of blended coals is close to that of the high-reactivity coal and the burnout performance tends toward that of the low-reactivity coal. Ignition and burnout behavior of blended coals can be adjusted by blending different reactivity types of coals.

3.2.3. Effect of Oxygen Concentration. Practical coal combustion often occurs at low oxygen concentration. For example, the oxygen concentration in a boiler decreases from initial 21 vol % in fresh air to 3−4 vol % at the outlet of furnace. For many advanced swirl burners, an intense recirculation of hot combustion products to the primary reaction zone rapidly dilutes the oxygen significantly to form a low oxygen concentration. However, the research on combustion characteristics of coal at low oxygen concentration is still very insufficient, especially for blended coal combustion at low oxygen concentration.

In this study, the combustibility index S is used to describe the effect of oxygen concentration on combustion characteristics of blended coals, which is a better method to reflect both ignition and burnout of blended coals. The index S is defined as follows:[24]

$$S = \frac{(dw/dt)_{max}(dw/dt)_{mean}}{T_i^2 T_b} \quad (2)$$

where $(dw/dt)_{max}$ is the maximum rate of weight loss and $(dw/dt)_{mean}$ is the average rate of weight loss, both in milligrams per minute.

Figure 7 shows the relationship between combustibility index S and mixture ratio at various oxygen concentrations. It can be seen that comprehensive combustion characteristics of blended coal decrease dramatically with decreasing oxygen concentration. The result is similar to that obtained by Li and co-workers[16] who claimed that the mass loss process on TGA curves shifts to

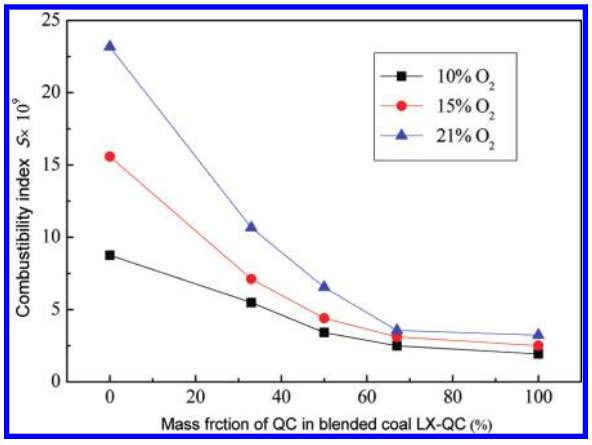

Figure 7. Change of index S with mixture ratio for different oxygen concentrations.

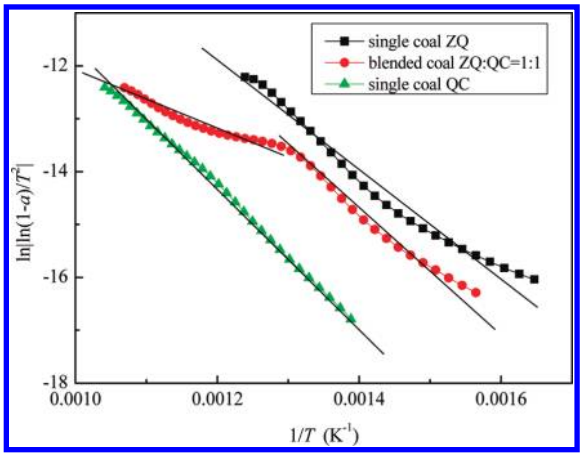

Figure 8. Kinetic analysis curves of individual and blended coal combustion.

a lower temperature when the oxygen concentration increases. Furthermore, the effect of oxygen concentration on index S is reduced gradually with increasing low-reactivity coal content, which means that oxygen concentration has greater influence on high-reactivity coal than low-reactivity coal. Consequently, the combustion characteristics of low-reactivity coal are less sensitive to the change of oxygen concentration than those of high-reactivity coal.

3.3. Kinetic Analysis of Blended Coal Combustion. *3.3.1. Coats−Redfern Method.* Coal combustion is quite complex and involves a range of chemical and physical processes, generally including devolatilization, combustion of volatiles, and char burnout. These concurrent processes contribute to the overall weight loss in thermogravimetric analysis. Therefore, the kinetic parameters derived from the relevant thermogravimetric curves should be considered as apparent values, which are not precisely related to any one particular mechanistic step.[32]

According to Arrhenius law,

$$\frac{d\alpha}{dt} = Ae^{-E/RT}f(\alpha) \tag{3}$$

$$f(\alpha) = (1-\alpha)^n \tag{4}$$

where $\alpha = (m_0 - m)/(m_0 - m_\infty)$ is the conversion fraction obtained from TG/DTG curves, of which m_0, m_∞, and m represent the initial, ultimate and the instantaneous weight (milligrams) of sample, respectively; t is the time, in seconds; E is the apparent activation energy, in kilojoules per kilogram; T is the temperature, in kelvins; A is a pre-exponential factor that includes the effect of partial pressure of oxygen, which is assumed to be constant; and n is the reaction order.

In the thermogravimetric experiments, a linear heating rate $\beta = dT/dt$ is used to represent the heating rate. So eq 3 can be transformed as follows:

$$\frac{d\alpha}{f(\alpha)} = \frac{A}{\beta}e^{-E/RT}\,dT \tag{5}$$

The Coats−Redfern integral method, which is one integral method for a single heating rate[33−35], is used widely in analyzing the kinetic parameters of nonisothermal combustion processes and was adopted in the present investigation. According to the Coats−Redfern equation:[36]

$$\text{if } n \neq 1, \quad \ln\left|\frac{1-(1-a)^{(1-n)}}{T^2(1-n)}\right| = \ln\left[\frac{AR}{\beta E}\left(1-\frac{2RT}{E}\right)\right] - \frac{E}{RT} \tag{6}$$

$$\text{if } n = 1, \quad \ln\left|\frac{\ln(1-a)}{T^2}\right| = \ln\left[\frac{AR}{\beta E}\left(1-\frac{2RT}{E}\right)\right] - \frac{E}{RT} \tag{7}$$

In order to obtain kinetic parameters, coal combustion is assumed to be a first-order reaction.[33] Therefore, the data in Coats−Redfern kinetic analysis were obtained by taking the reaction order as unity. The Coats−Redfern equation above is used to calculate the activation energy E and pre-exponential factor A. Thus a plot of $\ln|\ln(1-\alpha)/T^2|$ versus $1/T$ should result in a straight line with the slope equal to $-E/R$ for first-order kinetics.

From Figure 8, it can be noted that there is only one stage for analysis curves of individual coal combustion kinetics. However, kinetic analysis curves of blended coal combustion can be divided into two stages clearly. Therefore, kinetic parameters of blended coal combustion should be obtained by segmenting to avoid significant deviations. In this study, blended coal combustion is divided into two stages: low-temperature zone (T_i−T_e) and high-temperature zone (T_e−T_b). For both temperature zones, the Coats−Redfern method above is used to obtain kinetic parameters, apparent activation energy E, and pre-exponential factor A. The mean activation energy (E_m) proposed by Cumming is used to describe the reactivity or combustibility of blended coal combustion.[33,37] The method is shown as follows:

$$E_m = \sum E_i F_i \tag{8}$$

where E_i is the activation energy of different stages, in kilojoules per kilogram, and F_i is the mass loss fraction of the different stages, as a percentage.

Table 5 shows the kinetic parameters of blended coal ZQ/HX. It can be seen that kinetic parameters obtained from different temperature zones are quite different, which is consistent with the results achieved by Xu et al.[33] Because chemical bond-breaking and hydrogen-bond production of coal combustion at

dx.doi.org/10.1021/ef200686d |*Energy Fuels* 2011, 25, 3634–3645

Table 5. Kinetics Parameters of Blended Coal ZQ/HX Calculated by Coats−Redfern Method

temp zone (°C)	mass loss (wt %)	E_i (kJ·kg^{-1})	A_i (s^{-1})	correlation coefficient R^2
ZQ, E_m = 85.94 kJ·kg^{-1}				
334−536		85.94	358 890.71	0.9882
ZQ/HX = 5:1, E_m = 75.61 kJ·kg^{-1}				
341−555	74.45	77.73	73 931.00	0.9918
555−595	3.57	31.41	27.93	0.9996
ZQ/HX = 2:1, E_m = 75.41 kJ·kg^{-1}				
347−540	65.54	79.72	83 061.72	0.9949
540−607	11.36	50.50	573.98	0.9993
ZQ/HX = 1:1, E_m = 75.27 kJ·kg^{-1}				
356−534	56.49	79.92	69 172.46	0.9957
534−615	18.74	61.26	2771.72	0.9983
ZQ/HX = 1:2, E_m = 80.05 kJ·kg^{-1}				
364−522	44.90	82.58	90 915.04	0.9970
522−620	29.23	75.55	23 518.24	0.9989
ZQ/HX = 1:5, E_m = 83.96 kJ·kg^{-1}				
374−512	31.73	82.94	65 451.35	0.9980
512−627	40.49	84.76	81 936.35	0.9991
HX, E_m = 90.89 kJ·kg^{-1}				
390−630		90.89	173 731.54	0.9980

low temperatures need more energy,[38] both activation energy E and pre-exponential factor A in the low-temperature zone are much higher than those in the high-temperature zone. Moreover, mineral matter may play a catalytic role in blended coal combustion in the high-temperature zone. In addition, correlated coefficients of coal combustion in the high-temperature zone are all higher than those in the low-temperature zone, which indicates that the combustion in high temperatures is much closer to a first-order reaction.

It can also be seen from Table 5 that the mean activation energy of blended coal combustion may be even less than either of the activation energy values of individual coals, which cannot be calculated by weighed average method according to the activation energy values of individual coals and mixture ratio. Thermogravimetric experimental results show that the reactivity of blended coal increases with the increase of high-reactivity coal. The activation energy of blended coal combustion in the high-temperature zone accords with the same rule, while the mean activation energy of the whole combustion process differs clearly from it, as shown in Table 5. Hence, combustion reactivity of blended coals cannot be judged only by the activation energy derived by Coats−Redfern method due to the interaction between individual coals.

3.3.2. Kissinger−Akahira−Sunose Method. The single heating rate methods, like the Coats−Redfern method mentioned in section 3.3.1, require prior knowledge of the reaction mechanism, which is usually difficult to obtain. On the contrary, isoconversional methods do not require a prior assumption and mathematical model fitting for obtaining the kinetic parameters, which are called "model-free" methods. These methods require only a set of experimental data obtained at more than two different heating rates. Hence, isoconversional methods have been widely applied recently.

Isoconversional methods can be generally categorized into two main groups. One is the integral method and relies on the temperature integral approximation, including the Kissinger−Akahira−Sunose (KAS) method[39−42] (sometimes called the generalized Kissinger method), the Flynn−Wall−Ozawa (FWO) method,[43−46] and the modified Coats−Redfern method.[37,43,47] The other is the differential method and uses a determination of the reaction rate at an equivalent stage for various heating rates instead of any mathematical approximation. The Friedman method[48,49] is a well-known method of this type. The differential method avoids making any mathematical approximation but introduces some measurement uncertainties. Because the measurement of the conversion rate $d\alpha/dt$ is sensitive to the determination of the baseline and calibration of the thermal analysis equipment, it would be better to accept the limited but quantifiable deviation in the integral method rather than apply the differential method, in which the deviations are difficult to quantify.[42] Furthermore, there are more complex "model-free" methods, like the nonlinear "model-free" isoconversional method by Vyazovkin,[50,51] solutions of which can only be obtained by use of computer algorithms due to their complexity and nonlinearity. Therefore, the KAS integral method, which is one of the best-known integral methods, is also applied to compare with the Coats−Redfern integral method in our work.

By integration of eq 5, the following equation can be derived:

$$\int_0^\alpha \frac{d\alpha}{f(\alpha)} = \frac{A}{\beta}\int_0^T e^{-E/RT}\,dT = \frac{AE}{\beta R}\int_y^\infty \frac{e^{-y}}{y^2}\,dy \qquad (9)$$

where $y = E/RT$. Integrating in parts and truncating the series by assuming $y \gg 1$ results in the following temperature integral approximation:

$$\int_y^\infty \frac{e^{-y}}{y^2}\,dy \approx \frac{e^{-y}}{y^2} \qquad (10)$$

By taking the logarithm of eq 9 and using eq 10, we obtain the KAS equation:

$$\ln\frac{\beta}{T^2} = -\frac{E}{RT} + \ln\frac{AR}{E\int_0^\alpha \frac{d\alpha}{f(\alpha)}} \qquad (11)$$

$\int_0^\alpha d\alpha/f(\alpha)$ is a constant at a given conversion fraction α for different heating rates β. According to eq 11, plots of $\ln \beta/T^2$ versus $1/T$ at a given conversion fraction α should result in straight lines, with the slope of the straight lines equaling $-E/R$.

Figure 9 shows the relationship of conversion fraction α versus temperature T of blended coal ZQ/QC at different heating rates of 10, 15, 20, and 30 °C·min^{-1}. It can be observed that the combustion process of blended coal ZQ/QC is constituted of two stages, which is quite different from individual coals. Moreover, the conversion curves of the coal combustion process are shifted to a higher temperature zone and the reaction temperature at a given conversion fraction α increases with increasing heating rate. Dahiya et al.,[43] Sonobe and Worasuwannarak,[52] and Jankovic et al.[44] also obtained similar conclusions. This is due to more obvious thermal hysteresis at higher heating rates.

Figure 10 shows the plots of $\ln \beta/T^2$ versus $1/T$ at various conversion fractions α = 0.05, 0.10, 0.20, 0.30, 0.40, 0.50, 0.60, 0.70, 0.80, 0.90, and 0.95 according to the KAS method for

blended coal ZQ/HX = 1:1. For each given conversion fraction α and corresponding temperature, activation energy could be calculated from the slope of the plots of ln β/T^2 versus $1/T$. It can also be noted from Figure 10 that the linearity correlation of the fitting straight line is quite high, with correlation coefficients being generally above 0.99 in this study. Hence, the Kissinger−Akahira−Sunose (KAS) method is suitable in the study of blended coal combustion processes by thermogravimetry.

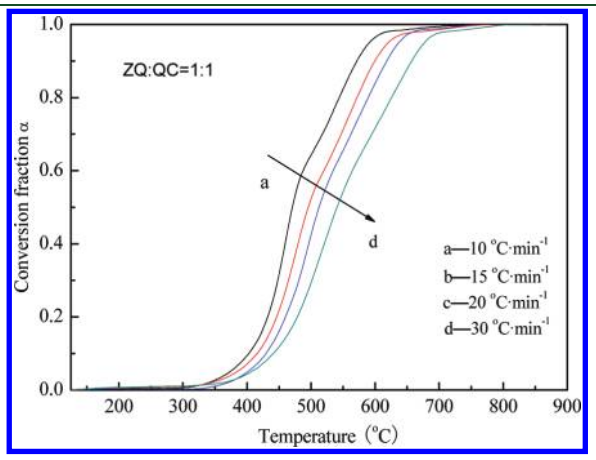

Figure 9. α versus T relationship of blended coal ZQ/QC at different heating rates.

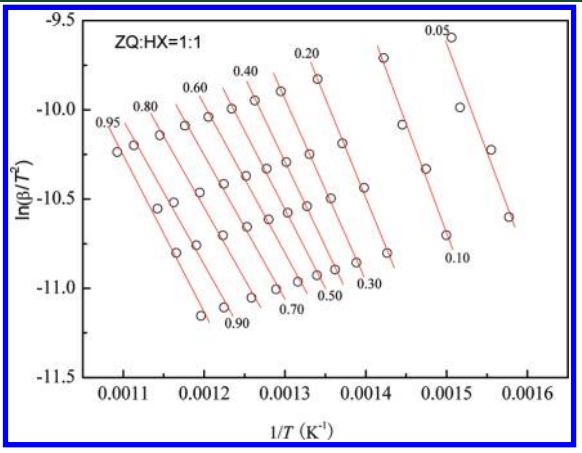

Figure 10. Plots of ln β/T^2 versus $1/T$ at various α for blended coal ZQ/HX.

Table 6 shows the apparent activation energy E_α and corresponding correlation coefficients at different degrees of conversion α for blended coal ZQ/HX and corresponding individual coals. From Table 6, we can find that E_α is not constant at different α and decreases with increasing conversion fraction. Combustion of blended coals is charactered by segmentation and the apparent activation energy in the low-temperature zone is higher than that in the high-temperature zone, which is consistent with results obtained by the Coats−Redfern method in section 3.3.1. Applying the average of E_α within α = 0.10−0.90 rather than the entire range was strongly recommended in our study, because most solid-state reactions are not stable at the beginning and ending periods.[44] Furthermore, correlation coefficients in the conversion range $0.10 \le \alpha \le 0.90$ are obviously higher than those in the conversion ranges $\alpha < 0.10$ and $\alpha > 0.90$ as shown in Table 6. The mean activation energy values E_m of individual coal combustion calculated by the KAS method are less than those obtained by the Coats−Redfern method. Nevertheless, it would be different for blended coals. It can also be observed from Table 6 that E_m of blended coal combustion calculated by the KAS method is between those of corresponding individual coals and increases with the content of low-reactivity coal, which is in accordance with TG/DTG experimental results. The mean activation energy obtained by the KAS method also shows nonadditive performance, which is consistent with results calculated by the Coats−Redfern method. Therefore, the KAS method (one of the isconversional methods) is more adequate than the Coats−Redfern method for analyzing the kinetics of blended coal combustion, because the Coats−Redfern method requires prior assumption of reaction mechanism and results calculated by the Coats−Redfern method sometimes differ clearly from experimental results.

4. CONCLUSIONS

In this paper, coal properties and combustion characteristics of blended coals in northwestern China have been investigated. Proximate and ultimate analyses, calorific value analysis, grindability,

Table 6. Kinetics Parameters of Blended Coal ZQ/HX Calculated by KAS Method

	ZQ		ZQ/HX = 2:1		ZQ/HX = 1:1		ZQ/HX = 1:2		HX	
α	E_α[a]	R^2	E_α	R^2	E_α	R^2	E_α	R^2	E_α	R^2
0.05	120.07	0.9761	107.21	0.9567	101.13	0.9671	107.15	0.9788	101.18	0.9643
0.10	110.53	0.9968	105.26	0.9943	101.66	0.9942	102.03	0.9954	99.89	0.9866
0.20	104.55	0.9999	98.67	0.9970	92.58	0.9977	93.36	0.9997	97.82	0.9974
0.30	89.99	0.9963	87.25	0.9967	84.69	0.9983	85.56	0.9996	94.04	0.9996
0.40	80.11	0.9933	79.97	0.9950	79.22	0.9995	80.10	0.9987	87.77	0.9999
0.50	71.67	0.9910	72.77	0.9919	73.48	0.9997	75.15	0.9978	80.81	0.9991
0.60	63.85	0.9893	65.71	0.9877	69.14	0.9944	70.83	0.9964	73.98	0.9985
0.70	56.85	0.9891	60.00	0.9829	67.13	0.9975	67.87	0.9948	68.32	0.9976
0.80	50.97	0.9892	61.09	0.9752	66.30	0.9974	65.04	0.9937	64.08	0.9965
0.90	47.91	0.9881	65.79	0.9744	67.15	0.9961	64.49	0.9917	61.54	0.9955
0.95	54.90	0.9610	74.01	0.9649	72.98	0.9678	69.90	0.9853	63.78	0.9930
E_m	75.16		77.39		77.93		78.27		80.92	

[a] E_α values are given in kilojoules per kilogram.

dx.doi.org/10.1021/ef200686d |*Energy Fuels* 2011, 25, 3634–3645

slagging properties, combustion characteristics, and kinetic analysis of blended coals are all investigated in detail.

Experimental results indicate that proximate, ultimate, and calorific value analyses of blended coals can be calculated by mass-weighted average of individual coals. Not all the HGIs of blended coals show additive behavior. Experiments are necessary to determine the grindability of blended coals. Blending a coal of high fusion temperature with a coal of low fusion temperature can significantly increase the ash fusion temperatures of blended coals in northwestern China. However, both the ash composition and fusion temperatures of blended coals show nonadditive performance due to the intense interaction of various mineral matters in blended coals.

Thermogravimetric experiments show that the intense combustion stage is quite different between blended coals and individual coals. All the thermogravimetric curves of blended coals lie between those of the corresponding individual coals, but not all are consistent with additive behavior. In addition, both volatile matter and ash contents have considerable effects on thermogravimetric curves of blended coals. The interaction effect of individual coals may delay the combustion process of high-reactivity coal. Competition for oxygen occurs between high- and low-reactivity coal. Moreover, the ignition performance of blended coals is close to that of the high-reactivity coal and the burnout performance tends toward that of the low-reactivity coal.

Kinetic analysis indicates the apparent activation energy of coal combustion is not constant at different conversion fractions and decreases with increasing conversion fraction. The combustion process of blended coals is charactered by segmentation, and the apparent activation energy in the low-temperature zone is higher than that in the high-temperature zone. The apparent activation energy of blended coal combustion calculated by the KAS method is between those of corresponding individual coals, while the apparent activation energy obtained by the Coats−Redfern method may be even less than either of the activation energy values of individual coals. The mean activation energy of blended coals shows nonadditivity performance in both KAS and Coats−Redfern methods due to the interaction between individual coals. Therefore, the KAS method (one of the isoconversional methods) is more adequate than the Coats−Redfern method for analyzing the kinetics of blended coal combustion, because the Coats−Redfern method requires prior assumption of reaction mechanism and its analysis results sometimes differ clearly from experimental results.

AUTHOR INFORMATION

Corresponding Author

*Tel +86-29- 82665185; fax +86-29-82668703; e-mail dfche@mail.xjtu.edu.cn.

ACKNOWLEDGMENT

This work has been financially supported by the Natural Science Foundation of China (50676076).

REFERENCES

(1) Jiang, Z. *J. Shanghai Jiaotong Univ.* **2008**, *42* (3), 345–359 (in Chinese).

(2) Su, S.; Pohl, J. H.; Holcombe, D.; Hart, J. A. *Prog. Energy Combust. Sci.* **2001**, *27* (1), 75–98.

(3) Peralta, D.; Paterson, N. P.; Dugwell, D. R.; Kandiyoti, R. *Fuel* **2001**, *80* (11), 1623–1634.

(4) Chi, T.; Zhang, H.; Yan, Y.; Zhou, H.; Zheng, H. *Fuel* **2010**, *89* (3), 743–751.

(5) Faúndez, J.; Arias, B.; Rubiera, F.; Arenillas, A.; García, X.; Gordon, A. L.; Pis, J. J. *Fuel* **2007**, *86* (14), 2076–2080.

(6) Osório, E.; de Lourdes Ilha Gomes, M.; Vilela, A. C. F.; Kalkreuth, W.; de Almeida, M. A. A.; Borrego, A. G.; Alvarez, D. *Int. J. Coal Geol.* **2006**, *68* (1−2), 14–29.

(7) Rubiera, F.; Arenillas, A.; Arias, B.; Pis, J. J. *Fuel Process. Technol.* **2002**, *77*−*78*, 111–117.

(8) Ikeda, M.; Makino, H.; Morinaga, H.; Higashiyama, K.; Kozai, Y. *Fuel* **2003**, *82* (15−17), 1851–1857.

(9) Wang, Q. Y.; Zhang, L.; Sato, A.; Ninomiya, Y.; Yamashita, T. *Fuel* **2008**, *87* (13−14), 2997–3005.

(10) Wang, Q. Y.; Zhang, L.; Sato, A.; Ninomiya, Y.; Yamashita, T. *Fuel* **2009**, *88* (1), 150–157.

(11) Vasko, F. J.; Newhart, D. D.; Strauss, A. D. *J. Oper. Res. Soc.* **2005**, *56* (3), 235–243.

(12) Gupta, A.; Das, A. K.; Chauhan, G. I. S. *Coal Prep.* **2007**, *27* (1−3), 28–38.

(13) Vuthaluru, H. B.; Brooke, R. J.; Zhang, D. K.; Yan, H. M. *Fuel Process. Technol.* **2003**, *81* (1), 67–76.

(14) Rubiera, F.; Arenillas, A.; Fuente, E.; Miles, N.; Pis, J. J. *Powder Technol.* **1999**, *105* (1−3), 351–356.

(15) Wang, J. H.; Chang, L. P.; Li, F.; Xie, K. C. *Energy Sources Part A: Recov., Util., Environ. Effects* **2010**, *32* (11), 1040–1051.

(16) Yanfen, L.; Xiaoqian, M. *Appl. Energy* **2010**, *87* (11), 3526–3532.

(17) Muthuraman, M.; Namioka, T.; Yoshikawa, K. *Fuel Process. Technol.* **2010**, *91* (5), 550–558.

(18) Muthuraman, M.; Namioka, T.; Yoshikawa, K. *Appl. Energy* **2010**, *87* (1), 141–148.

(19) Otero, M.; Gómez, X.; García, A. I.; Morán, A. *Chemosphere* **2007**, *69* (11), 1740–1750.

(20) Kok, M. V. *Energy Sources* **2002**, *24* (10), 899–906.

(21) Kok, M. V.; Pokol, G.; Keskin, C.; Madarasz, J.; Bagci, S. *J. Therm. Anal. Calorim.* **2004**, *76* (1), 247–253.

(22) Xie, K., *Structure and Reactivity of Coal*; Science Press: Beijing, 2002 (in Chinese).

(23) Riley, J. T.; Gilleland, S. R.; Forsythe, R. F.; Jr., H. D. G.; Hayes, F. J. 7th International Conference on Coal Testing, Charleston, SC, 1989.

(24) Sun, X., *Combustion experimental technology and method for coal-fired boiler*; China Electric Power Press: Beijing, 2001 (in Chinese).

(25) Zhong, D.; Qiu, J. *Power Syst. Eng.* **2003**, *19* (2), 13–14 (in Chinese).

(26) McLennan, A. R.; Bryant, G. W.; Bailey, C. W.; Stanmore, B. R.; Wall, T. F. *Energy Fuels* **2000**, *14* (20), 349–354.

(27) Lawrenc, A.; Kumar, R.; Nandakumar, K.; Narayanan, K. *Fuel* **2008**, *87* (6), 946–950.

(28) Plaza, P.; Ferens, W.; Griffiths, A. J.; Syred, N; Rybak, W. *Arch. Combust.* **2010**, *30* (3), 203–213.

(29) People's Republic of China, NDRC. *Performance design standard for furnaces and burners of large-capacity pulverized-coal-fired boilers*; China Machine Press: Beijing, 2004 (in Chinese).

(30) Kok, M. V. *J. Therm. Anal. Calorim.* **2005**, *79* (1), 175–180.

(31) Ma, B. G.; Li, X. G.; Xu, L.; Wang, K.; Wang, X. G. *Thermochim. Acta* **2006**, *445* (1), 19–22.

(32) Kok, M. V. *Energy Sources* **2003**, *25* (10), 1007–1014.

(33) Xu, Y.; Lin, s.; Yuan, H.; Zhu, K.; He, X.; Chen, G. *Challenges Power Eng. Environ.* **2007**, *3*, 153–156.

(34) Sutcu, H.; Piskin, S. *Combust. Sci. Technol.* **2009**, *181* (2), 264–273.

(35) Yorulmaz, S. Y.; Atimtay, A. T. *Fuel Process. Technol.* **2009**, *90* (7−8), 939–946.

(36) Coats, A. W.; Redfern, J. P. *Nature* **1964**, *201* (4914), 68–69.

(37) Cumming, J. W. *Fuel* **1984**, *63* (10), 1436–1440.

(38) de la Puente, G.; Marbán, G.; Fuente, E.; Pis, J. J. *J. Anal. Appl. Pyrol.* **1998**, *44* (2), 205–218.
(39) Kissinger, H. E. *Anal. Chem.* **1957**, *29* (11), 1702–1706.
(40) Kissinger, H. E. *J. Res. Natl. Bur. Stand.* **1956**, *57* (4), 217–221.
(41) Mittemijer, E. J. *J. Mater. Sci.* **1992**, *27* (15), 3977–3987.
(42) Starink, M. J. *Thermochim. Acta* **2003**, *404* (1−2), 163–176.
(43) Dahiya, J. B.; Kumar, K.; Muller-Hagedorn, M.; Bockhorn, H. *Polym. Int.* **2008**, *57* (5), 722–729.
(44) Jankovic, B.; Mentus, S.; Jelic, D. *Phys. B: Condens. Matter* **2009**, *404* (16), 2263–2269.
(45) Ozawa, T. *Bull. Chem. Soc. Jpn.* **1966**, *39* (10), 2071–2085.
(46) Flynn, J. H.; Wall, L. A. *J. Polym. Sci., Part B: Polym. Lett.* **1966**, *4* (5), 323–328.
(47) Burnham, A. K; Braun, R, L. *Energy Fuels* **1999**, *13* (1), 1–22.
(48) Friedman, H. L. *J. Polym. Sci., Part C: Polym. Symp.* **1964**, *6* (1), 183–195.
(49) Gupta, A. K.; Jena, A. K; Chaturvedi, M. C. *Scr. Metallurg.* **1988**, *22* (3), 369–371.
(50) Vyazovkin, S. *Anal. Chem.* **2010**, *82* (12), 4936–4949.
(51) Vyazovkin, S.; Wight, C. A. *Thermochim. Acta* **1999**, *341* (Sp. Iss.SI), 53–68.
(52) Sonobe, T.; Worasuwannarak, N. *Fuel* **2008**, *87* (3), 414–421.